# Detection of Seismic ULF Geo-Electrical Potential Variations as Tremor Precursors Prior to Quarry Blasts.

A.A. Adetoyinbo[1], O.I. Popoola[1], O.S. Hammed[2*], and L.A. Sumonu[3]

[1]Department of Physics, University of Ibadan, Nigeria.
[2]Department of Physical Sciences, Bells University of Technology, Ota, Nigeria.
[3]Department of Pure and Applied Physics, Ladoke Akintola University of Technology, Ogbomoso, Nigeria.

*E-mail: hammedolaide@yahoo.com

## ABSTRACT

A seismic ultra low frequency geo-electrical signal recording instrument was set up in three different quarry sites in the south-western part of Nigeria. This research was embarked upon to detect geo-seismic electrical signals produced from the brittle upper crust during rock loading and fracture as a simulated earthquake precursor. The seismic electromagnetic signals emitting from the interior earth in analogical pattern and detected at the earth surface through the signal detectors were transmitted to a conditioning circuit which not only protected the recording instruments from transients caused by ionospheric disturbances but also attenuated the 50 or 60 Hertz frequency caused by high voltage power transmission lines. The spectral analysis of the ULF signals with sampling of 48 KHz recorded during rock loading and fracture in each of the stations revealed that the amplitudes of the signals decrease with increasing frequency. The geo-electrical potential signals associated with ULF waves were varying during deformation stages of crustal layers of rocks. These signals were recorded a few seconds before and after fracture of the rocks as systematic precursors to the main tremors observed in each of the stations and felt five (5) kilometers away.

(Keywords: geo-electrical, seismic, ultra low frequency, ULF, precursors, fracture)

## INTRODUCTION

Any underground mining activity can, and most likely will, generate seismic events (i.e. mining tremors, usually called rock bursts). Mining operations lead to disturbances in the natural stress field in surrounding rock masses and subsequent stress release through rock bursts takes place in volumes (within or near the mine) where the redistributed stress exceeds the strength of the rock. Rock bursts are experienced daily in many mining areas around the world e.g. in central Europe, South Africa, Australia, Canada and Nigeria.

Seismicity in mines has frequently been studied in order to identify precursors to intensive seismic activity in the mine. The transmission of geo-seismic electrical signal from the brittle upper crust to the earth surface as a seismic precursor to tremors associated with the rock extraction or mining in the quarry sites or mines has neither been investigated thoroughly nor well understood, hence the need for this study. A *precursor phenomenon* is one which occurs before a mainshock and is a part of a physical preparation for the main rupture, it does not simply mean "before" but it implies casual linkage to the mainshock (Wyss and Habermann (1998). Earthquake precursor phenomena which are based on Seismicity changes have been proposed by many investigators as precursors (Melnikov et al., 1996; Enescu and Ito, 2001, 2002; Huang et al., 2002; Monterroso, 2003; Nuannin et. al., 2005; Schorlemmer et al., 2003, 2004; Wiemer et al., 2005). For example, Melnikov et al. (1996) demonstrated strain precursors to induced Seismicity in the Khibiny apatite mines. Fajklewicz and Jakiel,1989; Nuannin et al., 2005, applied a microgravity method to predict the occurrence of mining tremors, bursts and direction of migration of increased elastic strain in the rock masses. They found that negative changes of gravity micro anomalies signaled approaching mining tremor. Holub (1996) investigated space-time variations of the frequency-energy relation for mining-induced Seismicity in the Ostrava-Karvina mine district (Czech Republic).

A major component in attempts to study and possibly forecast characteristics of rock bursts includes the deployment of seismic monitoring networks covering the respective mine. Such networks can detect, locate and quantify the tremors and so provide data for further analysis. Routine seismic monitoring in mines was introduced about 40 years ago with two major objectives: Firstly, to locate major seismic events and thus guide rescue operations; Secondly, to detect the potential instabilities. In 1988, the world's first mine-worthy digital seismic data acquisition was introduced by Mendecki et al. (1990) in South Africa. The system enabled the implementation of real time quantitative seismology as a management tool for continuous monitoring of the rock mass response to mining. Seismic monitoring consists of data acquisition, seismological processing and interpretation in terms of potential for large instabilities.

## SEISMO-ELECTRICAL SIGNALS

Seismo-electrical signals (SES) are anomalous changes in the electric potential measured by electrical dipoles from which there is no simultaneous variation in the earth's magnetic field. SES includes electrical, magnetic and electromagnetic (EM) signals with frequencies from DC to megahertz frequencies, generated in the upper crust. The number of mechanisms proposed to explain these phenomena include piezoelectricity, contact electrification, exoelectron emission, streaming potential, EM excitation of water droplets and fault zones acting as EM waveguides.

These types of observation and explanations are the basis of emerging research into the use of electrical signals as pre-earthquake indicators and fluid flow monitors. In this present research, we concentrated on the seismic electrical signals produced from the brittle upper crust during rock loading and fracture to simulate earthquake precursors. Derr (1973) collated the evidence that there are electrical disturbances generated from quartz crystals in the rock deformation. A radio emission of $2.56 \times 10^{-6}$ W Hz$^{-1}$ total spectral power was observed six days before the great Chilean earthquake of 1960, on a network of widely spaced radio receivers in Colorado (Warwick et al., 1982). This EM signal, was explained using a mechanism involving stress induced fracture of quartz-bearing rocks. This signal was also reproduced by means of a

theoretical model incorporating pressure variations and fluid saturation (Kligfield et al., 1986).

Numerical calculations were applied to model reasonable mechanisms for EM propagation within the earth's interior (Sumitomo, 1994), such as the radio emissions of Warwick et al. (1982). The deviations between model predictions and field results suggest difficulties in detection, which arise due to interference of EM waves from natural and artificial sources. Using telluric currents allows more realistic predictions to be made and may offer a more reliable signal for monitoring. DC electrical potential signals have since been measured in seismically sensitive areas around volcanoes (Haartsen et al., 1998) and preceding earthquakes, when precursors of 40mV (Meredith et al., 1990) and 90mV (Corwin and Morrison, 1977) were reported.

The dilatancy-diffusion hypothesis for earthquakes (Scholz,1996) can be employed as an interpretative tool for electrical signals recorded in seismic areas. The fluid flow occurring in these areas is due to the build up of critical pressure compartments (Byerlee, 1993) which rupture when hydrostatic pressures exceed the lithostatic pressure. This fluid flow carries electrical currents generating electrical signals, commonly referred to as streaming potentials (SP). Fenoglio et al. (1995), using this model, calculated magnitudes of electrical and associated magnetic signals which show quantitative agreement with magnetic signals recorded prior to the magnitude 7.1 Loma Prieta 1989, earthquake.

## THE MECHANICS OF ROCK DEFORMATION

### Porous Media and Surface Roughness

The porosity (f) of a rock sample is a controlling factor in transport (David, 1993), mechanical (Dunn et al, 1973) and acoustical properties (Ayling et al., 1995) of rocks and is defined as the pore volume per unit rock volume. The initial value is dependent on grain size and distribution, initial deposition conditions, secondary porosity alteration methods and of course on the rock type. The specific surface area (Sc) of a porous medium is defined as the pore surface area in a sample divided by the total volume of the sample. It depends on the grain packing type and is found to be equal to $S = 3(1-f)/R$ for 'spherical' grains where R is the grain radius.

The surface area can be correlated to permeability (Walsh and Brace, 1984) which stems from the fact that it is inversely proportional to capillary size. Another mechanics of rock deformation is the surface roughness of the rocks. In reality, rock surfaces and associated fractures are always rough and exhibit scale invariance (Brown and Scholz, 1985a). This roughness affects the properties of the rock. For example roughness affects the hydraulic properties of the flow system by increasing frictional resistance to flow and by channeling of flow along fracture surfaces. It also affects the transport properties of a medium by changing the dimension of the flow paths that particles take (Glover et al., 1998), as well as by increasing the total area available on the fracture surface for chemical reactions.

In addition to the hydraulic properties, roughness, including asperity distributions, affects the shear strength and the compressibility of rocks. The roughness of pore surfaces of sandstones on microscopic levels has been shown to be fractal over four orders of magnitude (Katz and Thompson, 1985) and the fractal relationships allow accurate predictions of electrical conductivity (Katz and Tugman, 1988). The authors suggest this self-similarity is produced through steady state crystal growth during rock formation. However the inclusion of a fractal description of surfaces in models of electrical conductivity is not always appropriate (Ruffet et al., 1995).

## Stresses

Two different types of forces act upon a continuous medium: body forces which are due to the acceleration due to gravity and surface forces acting on a particular surface area. The limiting value of the ratio $\partial F/\partial A$ as $\partial A$ approaches zero is called the stress vector at that point where F is an applied force and A is the area acted on by that force. Stress at a point is a second-order tensor, which means that it takes (in 3D space) nine components to describe, or six independent components for an isotropic homogeneous body.

The nine components required to identify the stress $(\sigma_{ij})$ at a point are represented in Figure 1a and expressed in matrix form in Equation 1.

$$\sigma_{ij} = \begin{bmatrix} \sigma_{11} & \sigma_{12} & \sigma_{13} \\ \sigma_{21} & \sigma_{22} & \sigma_{23} \\ \sigma_{31} & \sigma_{32} & \sigma_{33} \end{bmatrix} \quad (1)$$

Where $\sigma_{23}$ represents the stress component acting on the face normal to $X_2$ in the direction of $X_3$. If all possible stresses through a point are plotted then an ellipsoid known as the stress ellipsoid is obtained as shown in Figure 1b.
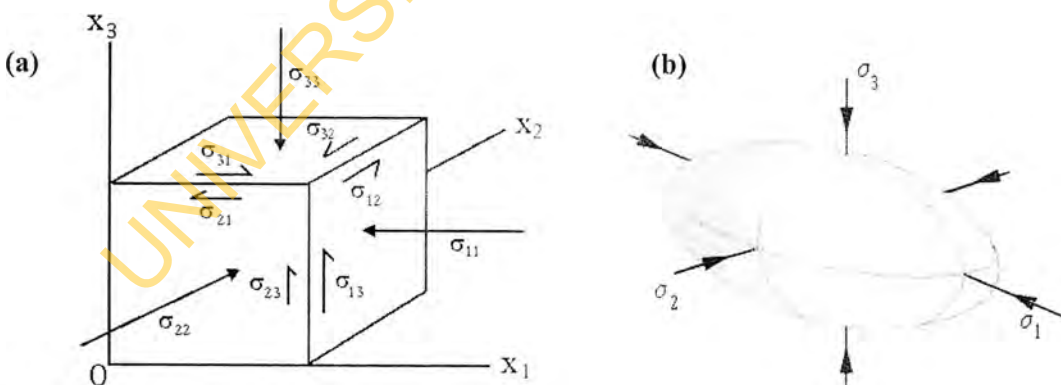


**Figure 1:** Schematic Diagrams Showing (a) Nine Stress Components Required to Describe Stress at a Point and (b) The Stress Ellipsoid Produced if all Possible Stresses Through a Point are Plotted.

Where $K$ is the bulk modulus of the rock frame containing pores and $k_s$ is the bulk modulus of the solid rock. Substituting Equation 9 into 6, 7 or 8 and providing that fluid pressure is fully communicated within the connected porosity, it is seen that the effective normal stresses that control crack growth, macroscopic fracture and friction are reduced by the magnitude of the fluid pressure.

The effective stress principle can be described graphically, using the experimental results shown in Figure 2. Zoback and Byerlee (1975) however found a value of $\delta_{ij} = 4$ in Berea sandstone from permeability measurements. This result suggests that the permeability is more strongly influenced by fluid pressure than confining pressure. Berryman (1992b) shows that these results cannot be explained using an 'equivalent homogeneous rock's model but in principle can be explained by a 'two-constituent homogeneous' paradigm for microscopically homogeneous rocks. For inhomogeneous rocks a rigorous analyses suggests that the pore fluid pressure is least effective at counteracting the changes caused by confining pressure.

Chemically, a reactive fluid at a certain pressure and temperature creates the conditions necessary for what is known as sub critical crack growth (Atkinson, 1982, Atkinson and Meredith, 1987) which involves crack extension occurring at a stress intensity value lower than critical stress intensity. The mechanisms responsible include stress corrosion, hydrolytic weakening and pressure solution, of which stress corrosion is the most heavily investigated. It is the weakening of strained molecular bonds by a chemically active fluid hence chemical reaction kinetics can be used to explain the dependence of crack growth rates in various environments (Freiman, 1984).

The relationship between the crack propagation velocity ($v_c$) and the normalized stress intensity factor $K$ consists of three regions. In the first region crack velocity is controlled by the stress corrosion rate while in region 2 the cracking rate is limited by the rate at which the chemically active fluids can reach the crack tip. Finally in region 3 the mechanical effects dominate and chemical effects are reduced considerably. A review of the experimental data concerning sub critical crack growth in a range of geological materials is given by Atkinson (1984).
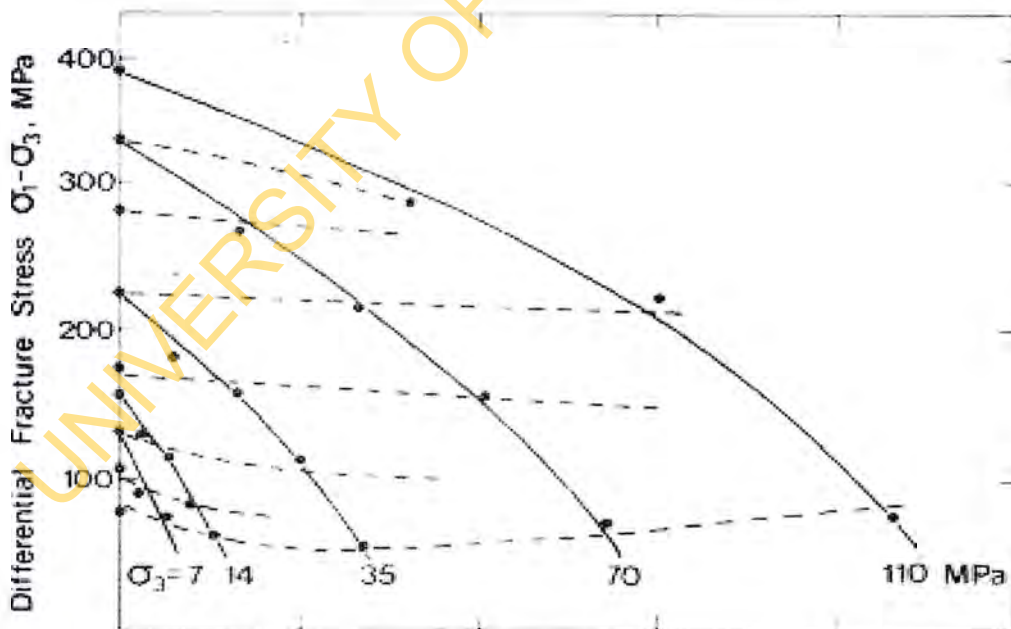


**Figure 2:** Influence of Pore Fluid Pressure on the Fracture Strength of Sandstone Under Triaxial Deformation. (The hashed lines are lines of constant effective stress as described by the effective stress law, equation 2-22 (Taken from Murrell, 1965)).

The stress tensor can be separated into an isotropic and deviatoric component (see Ranalli, 1995). The isotropic part is defined as

$$\sigma_{ij}^{\circ} = \tfrac{1}{3} \sigma_{KK} \delta_{ij} \qquad (2)$$

Where $\sigma_{KK}$ is the sum of the on-diagonal components of the stress tensor and $\delta_{ij}$ is the identity matrix which is equal to one when $i = j$ and zero when $i \neq j$. The deviatoric stress is defined by:

$$\sigma_{ij}^{i} = \sigma_{ij} - \sigma_{ij}^{\circ} \qquad (3)$$

Which determines the resultant stress when the isotropic part has been removed and is calculated using the off-diagonal components of the stress tensor.

The stress tensor can therefore be expressed as:

$$\sigma_{ij} = \tfrac{1}{3} \sigma_{KK} \delta_{ij} + \sigma_{ij} \qquad (4)$$

The principal stresses are an important representation of the stress state in structural geology and rock mechanics. When the principal stress axes are known, they allow a stress co-ordinate frame to be adopted. The principal axes are those where the only non-zero components of the stress tensor are the on-diagonal components and represent axes that define planes of no shear stress normal to them. The principal stresses are the values of the on-diagonal components. To determine the principal stress axes a suitable transformation must be found which reduces the stress tensor to a diagonal matrix,

$$\sigma_{ij} = \begin{Bmatrix} \sigma_{11} & \sigma_{12} & \sigma_{13} \\ \sigma_{21} & \sigma_{22} & \sigma_{23} \\ \sigma_{31} & \sigma_{32} & \sigma_{33} \end{Bmatrix}$$

$$T' = \begin{Bmatrix} \sigma_{11}^{p} & 0 & 0 \\ 0 & \sigma_{22}^{p} & 0 \\ 0 & 0 & \sigma_{33}^{p} \end{Bmatrix}$$

Where $\sigma_{ij}^{p}$ is the principal stress. The principal stresses are denoted by $\sigma_{1}$, $\sigma_{2}$ and $\sigma_{3}$ and the convention is used where compression is taken to be positive.

## Failure Modes during Experimental Triaxial Deformation

Rocks, under stress, fail in different ways depending on the temperature and pressure. At low temperatures and high strain rates, rocks are brittle-elastic. They deform elastically at stresses up to about 50% of their strength then crack propagation becomes dominant and eventually the rock fails as cracks coalesce to form a large fracture or failure surface (Jaeger and Cook, 1979). This occurs due to stress concentrations arising at crack tips leading to initiation and propagation of the cracks. A natural rock formation contains levels of pore fluid of varying salinity, temperature and pressure within the interconnected pore and crack network. The fluid can affect the rock both mechanically and chemically. Mechanically the rheological behavior of the rock then depends on the total macroscopic stress and pore pressure which creates important implications in large scale faulting (Hubbert and Rubey, 1968; Sibson, 1980). The concept gives rise to an effective pressure $\sigma_{ij}^{e}$ (Jaeger and Cook, 1979, Berryman, 1992a) defined as

$$\sigma_{ij}^{i} = \sigma_{ij} - p_{f} \delta_{ij} \qquad (5)$$

if the rock is fully saturated and where $\sigma_{ij}$ is the total macroscopic stress and $p_{f}$ is the pore pressure and $\delta_{ij}$ is a constitutive relation of poroelasticity called the effective stress coefficient. If the value of $\delta_{ij} = 1$, therefore for an incremental increase in the pore fluid pressure, the pore opens by the same amount as it would have given a decrease in the normal pressure on the fracture by the same amount. If $\delta_{ij} \neq 1$, then Nur and Byerlee (1971) show how it can be determined through the relationship:

$$\delta_{ij} = 1 - \frac{k}{k_{s}} \qquad (6)$$

## Permeability Changes

Permeability is one of the most important rock characteristics in relation to hydrocarbon production, geothermal recovery rates and radioactive storage procedures. It is measured using fluid flow techniques. The coefficient of permeability ($k$) in saturated media relates the fluid flux to the applied pressure gradient. This relation is quantified in Darcy's law, which states

$$q_x = -\frac{k}{\eta}\frac{dP}{dx} \qquad (7)$$

where $q$ is the Darcy velocity and $\eta$ is the viscosity of the fluid in the x-direction. Since dimensional analysis reveals $k$ to have units of $m^2$, the permeability can be thought of as an effective cross-section for flow. This equation is valid only for $R_e \ll 1$ where $R_e$ is the Reynolds number given by:

$$R_e = \rho v l \Big/ \eta \qquad (8)$$

Where $\rho$ is the fluid density and l is a characteristic length of the pore space.

Transport properties such as permeability and electrical currents are dependent on the connected pore space in the rock. It is known that increasing normal and effective stress closes pores and micro cracks in intact granites (Batzle et al., 1980), jointed granites (Brown and Scholz, 1986) and that this closure affects the fluid flow rate in fractures (Tsang and Witherspoon, 1981). For example the model used by Glover et al. (1998) shows how the mean aperture of a synthetic fracture can close by 5 orders of magnitude with a closure pressure of 13.5MPa. The measurement of $k$ therefore reveals much information about the shape of pores and cracks in rocks. These effects will therefore affect the permeability of a rock. An increasing confining pressure reduces $k$ through porosity reduction. These effects are summarized in Equation 22 (Scheidegger , 1974) for a capillary model

$$k = c\frac{\phi^3}{s_i^2 \tau^2} \qquad (9)$$

where $S_i^2$ is the specific internal area, $t$ is the tortuosity, $f$ is porosity and c is a constant dependent on pore geometry.

Permeability is reduced due to porosity closure during compaction (Trimmer et al., 1980) and increased significantly due to microcrack opening and formation during dilatancy. These studies relate to crystalline rocks and are generally accepted. In sedimentary rocks permeability evolution is considered more complex, (Zhu and Wong, 1996; Keaney, 1998) resulting in permeability decreases during dilatancy. Network models consisting of tubular pores and stress induced cracks can adequately describe this behavior (Zhu and Wong, 1996) and without regard to network dimensionality or pore radii distribution (Bernabe and Bruderer, 1998).

## EXPERIMENTAL PROCEDURE

A complete standardized geo-seismic electrical signal recording station was set up in each of the three selected quarry sites or locations in the south-western part of Nigeria. This research was embarked upon to detect seismic electrical potential signals produced from the brittle upper crust during rock loading and fracture as a simulated earthquake precursor. The recording instruments were strategically stationed at these different locations. These stations A, B, and C are crustal rocks extracting Quarries located at Ibadan, Abeokuta, and Ijebu-Ode, respectively, which are in south-western part of Nigeria. Each of these stations was equipped with a data acquisition unit that comprises the detector array (8 parallel connected copper clad earth rods and one grounded copper rod), seismic ultra low frequency (ULF) signal receiver, a 16-bit analog to digital interface card, data computer, high resolution multimeter, magnetic compass, measuring tape of 200 meters capacity, 9 copper clamps, earth wire of diameter 2.5 millimeter and length 100 meters, RG 59 Coaxial cable of resistance 75Ω and length 150meters, and 3 dual line jack plugs. Details of how the ULF signal receiver was fabricated by the Authors are described in Adetoyinbo et al. (2008).

The magnetic compass was used to determine the magnetic orientation of each of the stations. The magnetic North and South of the site in each of the stations were located. Four copper clad earth rods of eight (8) feet in length were driven into the ground of depth eighteen (18) inches

towards the magnetic North of the site which serves as Earth probe 1 as shown in Figure 3. These rods were spaced, 20 feet apart from one another and connected in parallel with the aid of earth wire and copper clamps. A distance of fifty (50) meters was measured out with the aid of the measuring tape from the Earth probe 1 to the South direction which serves as the Earth probe 2 and the procedure carried out in the Probe site 1, was repeated in the Probe site 2.
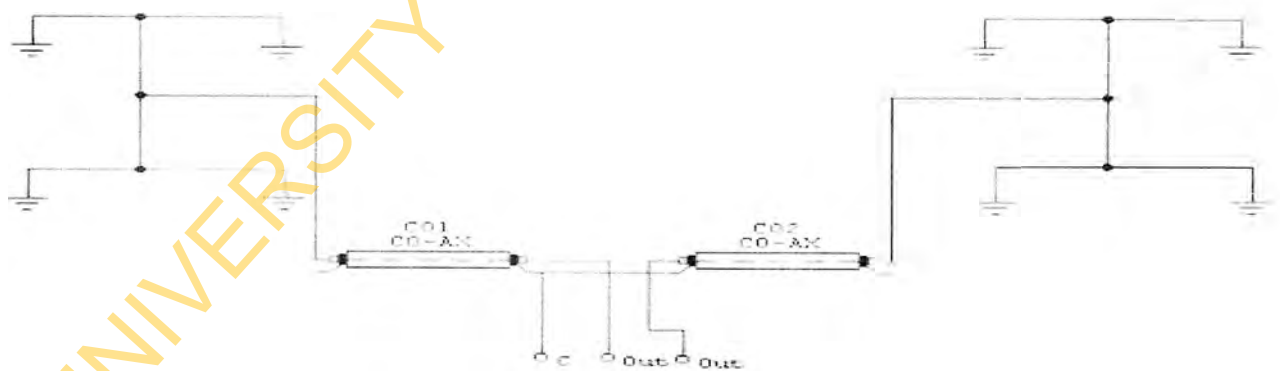


**Figure 3:** A Photograph Showing the Parallel Connection of Copper Clad Earth Rods Driven to the ground as ULF Signal Detectors that formed Earth Probes in Quarry Site.

The two widely spaced earth probe terminals were connected via center conductor of the coaxial cable (as shown in Figure 4.) to the dual line Jack plug 1 while the outside shield of the cable of each of the terminals were connected together and grounded through an earth rod. The jack plug 1, serves as the input to the ULF signal receiver. The dual line Jack plug 2, links the output of the receiver, via Jack plug 3, to the input of high resolution multimeter and the interface card (sound blaster card driver) implemented in the computer. The blaster card post filters and converts the signals from the analog to digital.

For proper analysis of the data obtained in the system, spectrum lab software (sound blaster card driver) was installed in the hard disk of the computer. In each of these stations, fifty (50) wells or holes, each of diameters 6 centimeters and 15 meters deep, were drilled down the crustal layers with the aid of a hydraulic drilling machine shown in Figure 5, and later filled with the explosives and detonators.

The rocks were mined by means of explosion, in rapid succession, on 50 charges of explosive wells, filled from the bottom to a height of 10 meters



**Figure 4:** Schematic Diagram of the Parallel Connection of Copper Clad Earth Rods Driven to the Ground as ULF Signal Detectors that formed Earth Probes in Quarry Sites.
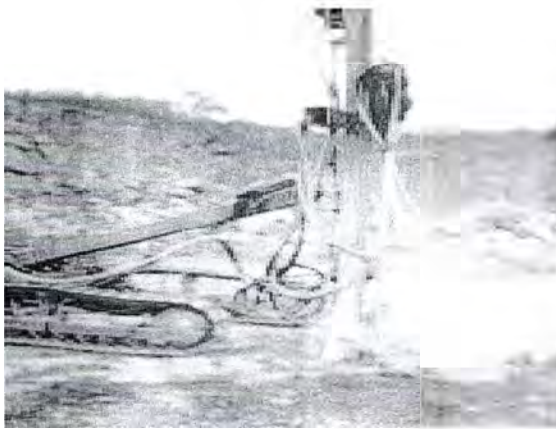
**Figure 5:** A Photograph Showing a Hydraulic Drilling Machine used to Drill Holes down the Crustal Layers during the Rock Blasting Process in Quarries.

The recordings began few seconds before the explosions and the desired signals (ULF electromagnetic waves) were recovered from the earth through the signal detectors (earth rods) stationed at a distance of one (1) kilometers from the wells with the explosives during the extraction or mining of the rocks. These signals were then directed via coaxial cables to a conditioning circuit in the seismic ULF signal receiver. The signals then passed through a circuit which removed any ground loop problem which may occur at the computer interface during blasting of the rocks in Quarry sites. With this arrangement, Amplitude, Frequency and Geo-electric potential changes of the signals with time during rock loading and fracture in the quarry sites were recorded.

## RESULTS AND DISCUSSION

The recordings began few seconds as the wells drilled down the crustal layers were being stressed or loaded with the aid of blasting materials and techniques. The seismic electromagnetic signals emitting from the interior earth in analogical pattern and detected at the earth surface through the signal detectors were transmitted to a conditioning circuit which did not only protect the recording instruments from transients caused by ionospheric disturbances but also attenuated the 50 or 60 Hertz frequency caused by the commercial power. We recorded only the Ultra-low frequency part of the Electromagnetic spectrum because this is the highest frequency that reached the earth's surface with little attenuation probably due to its huge wavelength.

The analogical recordings were digitized through the sound blaster card (interface card) implemented in the data computer with the aid of a spectrum lab software. The digitization of analog signals recovered from the earth is imperative because of the tendency of analog signals to corrupt easily even with just a little interference of noise signals during the transmission or storage processes. The results obtained in each of the stations showed that the explosions in the wells did not occur simultaneously but in rapid succession from the bottom to the top and from the first well to the last one, though this led to the uniform collapse of the parental rocks in the crust. It is this uniform collapse that generated the recorded seismic ULF electromagnetic waves of unique large impulsive signals at the fracture state of the lower crustal layers.

The spectral analysis of the ULF signals with sampling of 48 KHz recorded during rock loading and fracture in each of the stations (as shown in Figures 6, 7, and 8) revealed that the amplitude of the signals decreases with increasing frequency. This explains why the radio seismic signals have a typical maximum intensity in the low frequency and minimum intensity in the higher frequency at times up to 20 KHz in the strongest signals. Thus this prevented these signals from interfering with radio communication.

The geo-electrical potential signals associated with the ULF waves were varying anomalously during deformation stages of crustal layers of rocks. These signals were recorded a few seconds before and after fracture of the rocks ( as shown in Table 1) as systematic precursors to the main tremor observed in each of the stations and five (5) kilometers away. This implies that the rock fracture associated with each of these recording stations is a gradual process formed through the initial formation of micro fracturing which leads to the sudden formation of some macro-fractures and to final collapse of the loaded or stressed rocks. The culminating fracture sequence is not impulsive but a combination of macro and micro structural events which condition the final collapse.
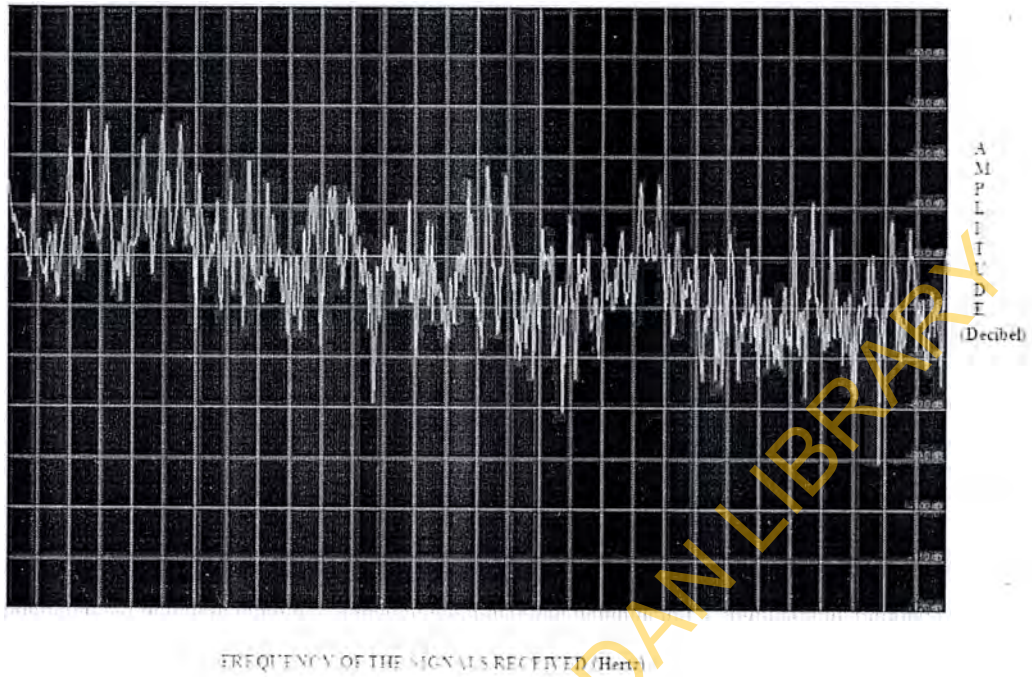
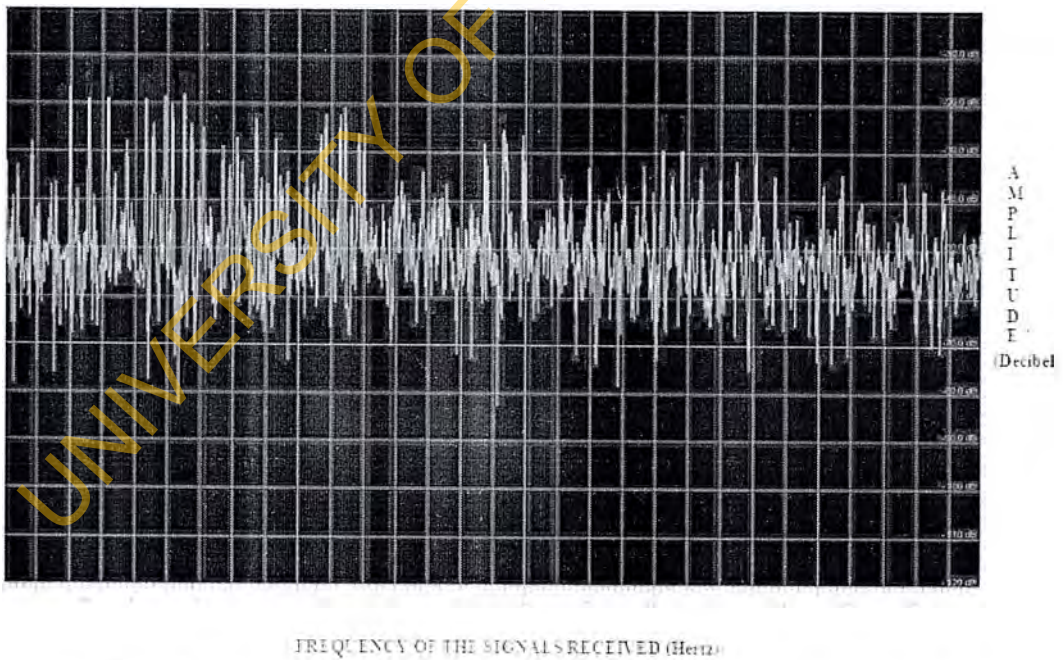**Figure 6:** A Spectrum Graph Showing ULF Emitted and Recorded in Station A.



**Figure 7:** A Spectrum Graph Showing ULF Emitted and Recorded in Station B.
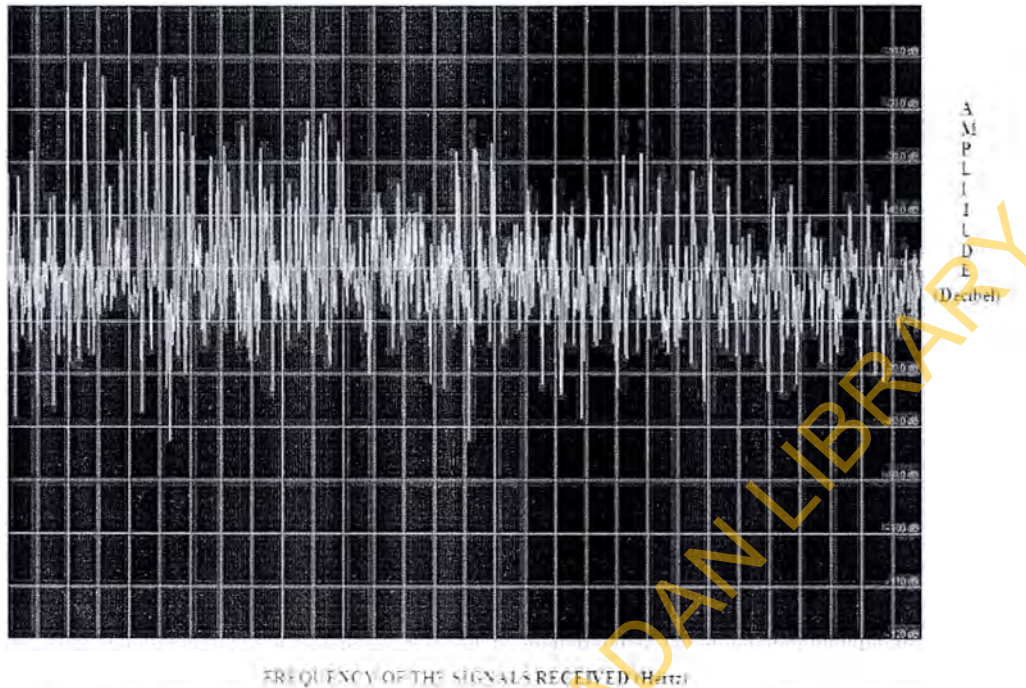
**Figure 8:** A Spectrum Graph Showing ULF Emitted and Recorded in Station C.

A sharp increase in peak value of geo-electrical potential changes was observed immediately at fracture stage, at 11, 15, and 18 seconds in the stations A, B, and C respectively after which a decrease to a constant value was observed during stable sliding on a macroscopic fault plane as shown in Figures 9, 10, and 11. This signifies that the macroscopic shear fault is acting as an enhanced current path or channel.

The highest peak value of geo-electrical potential changes recorded in Station C, may, probably, imply that the station lies on a wider macroscopic fault plane which paves way for large enhanced current path and consequential large electrical signals. The data analysis of the geo-electrical potential changes recorded revealed that geo-electrical potential variation depends on the mode of deformation of crustal layers and therefore the resulting electrical signals might be used as a measure of structural damage, in the crust, manifested through these processes This result recognizes the possibilities of geo-electrical potential delineating the fractured media as confirmed by Al-saigh et al., 1994, that the measurement of

self-potential at different stages of deformation could be found useful in delineating structural damage or inversely predicting the stress state of the crust.

The large volume of geo-electrical potential variation that was observed prior to the point of fracture of the crustal rocks during rock loading implies that the earth crust exhibits an elastic property, being a brittle medium, when stressed. This result showed that the state of stressing or loading the crust corresponds to the emission of geo-electrical potential variations that accompanied the ULF waves.

The higher the stressing or loading state of the crustal layers, the more the emission of ULF waves and transmission of geo-electrical potential signals reaching the earth surface. This is in concurrence with the model of Yosida et al. (1997), which verified that a large instantaneous stress drop during dynamic fracture and slip within the crust produces an effective polarization in the quartz crystals which when summed up, all the quartz crystals present are detectable on the Earth surface.
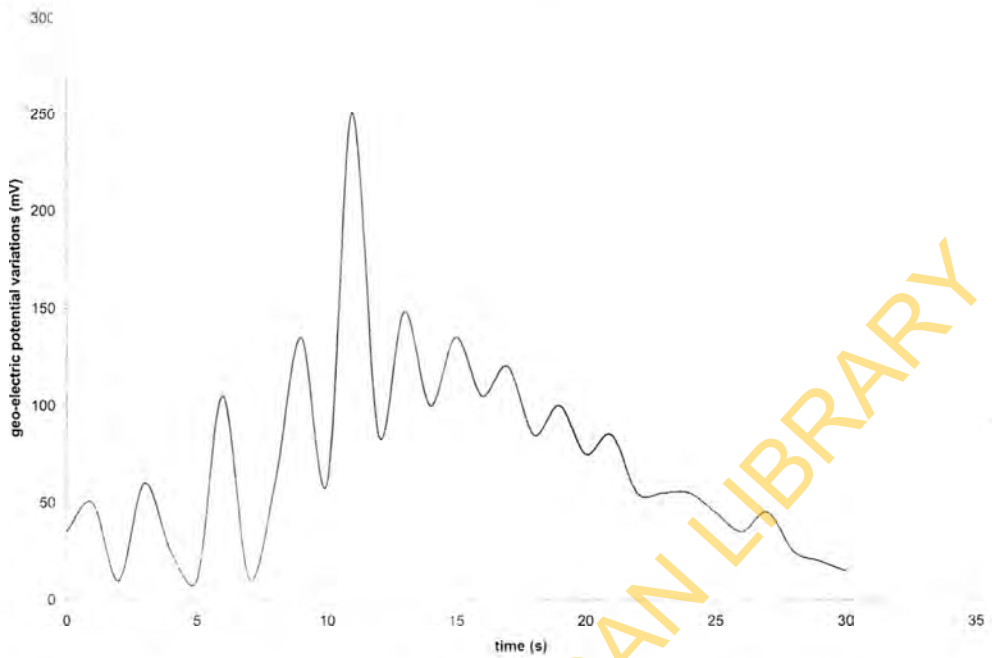
**Figure 9:** Showing Geo-Electrical Potential Signals Recorded during Rock Loading and Fracture in Station A.
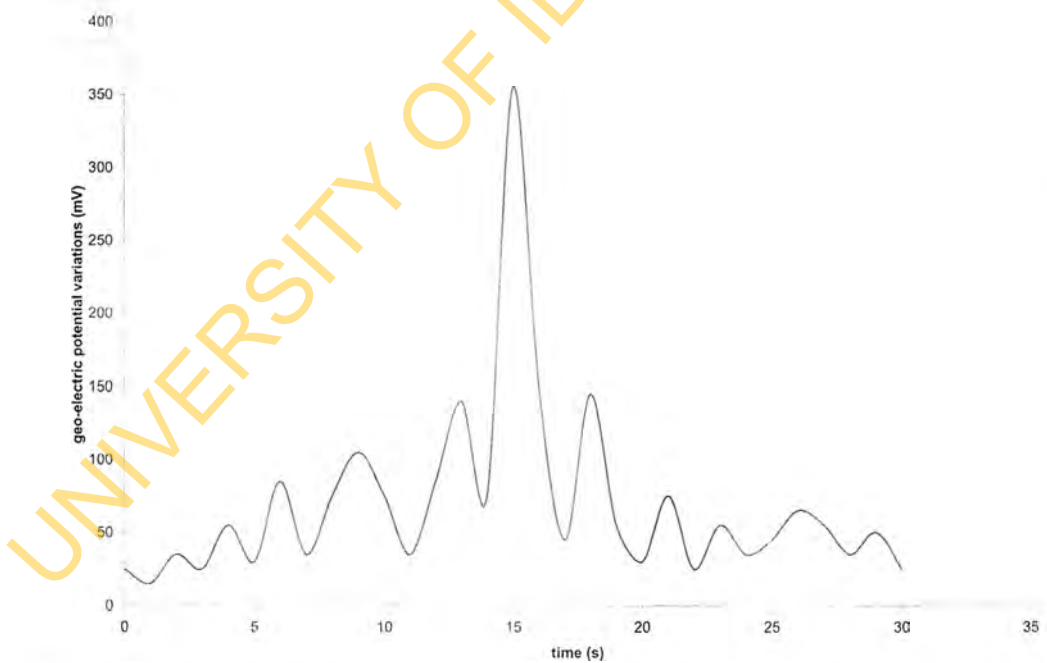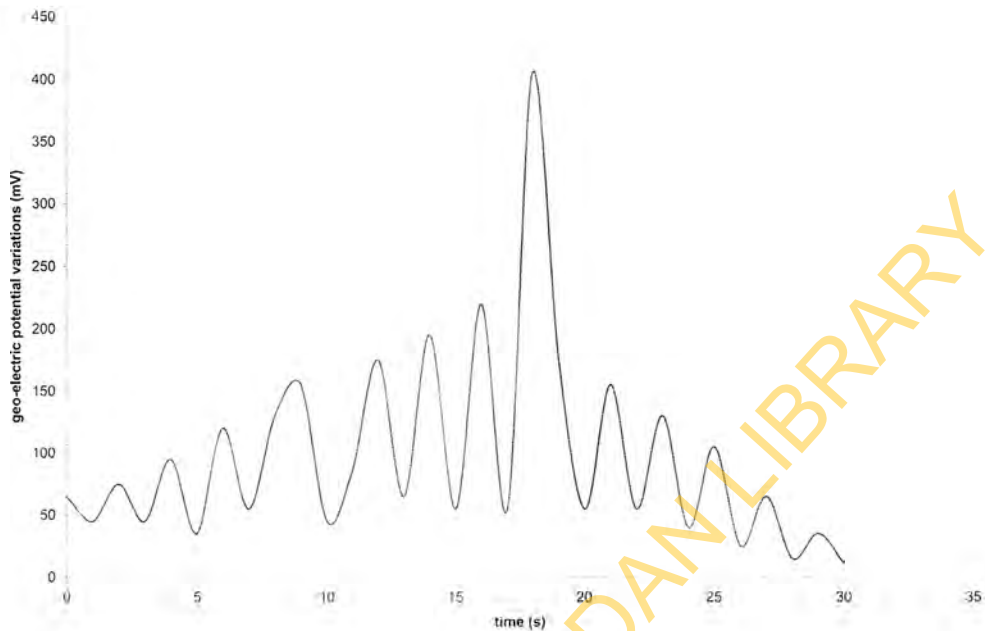


**Figure 10:** Showing Geo-Electrical Potential Signals Recorded during Rock Loading and Fracture in Station B.

**Figure 11:** Showing Geo-Electrical Potential Signals Recorded during Rock Loading and Fracture in Station C.

A previous study by Yosida et al. (1994), shows that the geo-electrical potential signal variations generated from the crust are due to the dynamic stress drop and not frictional slip on the fault plane, although shear movements in quartz crystals are known to produce piezoelectric signals.

The radio seismic emission of large volume of geo-electrical potential signals recorded few seconds prior to the fracture serves as a systematic precursor that precedes a tremor or earthquake of low magnitudes associated with seismic activities in the Quarries. The occurrence of this radio seismic precursor may be due to the formation of micro-fractures which break the chemical bond binding the rock layers and cause an unbalance in the distribution of electric charges. This conforms with the Mognaschi hypothesis that when a material is not a conductor, the fracture would separate the free charges, therefore, generating an electric field which in turns would create an electric micro-discharges between the rock layers with a consequent electromagnetic emission.

## CONCLUSION

It can be deduced on the basis of our findings that the state of stressing or loading the earth crust corresponds to the emission of geo-electrical potential signals that accompanied the ULF waves. The higher the stressing state of the crustal layers, the more the emission of ULF waves and the transmission of geo-electrical potential signals reaching the earth surface. The geo-electrical potential signals vary significantly with time during rock loading and increase sharply at the fracture state of the rocks in the earth crust.

We can conclude that the radio seismic emission of large volume of geo-electrical potential signals recorded during the rock extraction or mining in this research, though on a microscopic scale, prior to the rock fracture serves as a systematic precursor that precedes a tremor or simulated earthquake of low magnitude associated with seismic activities in the quarries. On a macroscopic scale, in the active fault zones, this can be a way towards the earthquake prediction.

**Table 1:** Values of Geo-Electrical Potential Signals with Time Recorded during Rock Loading and Fracture in the Three Stations, A, B, and C.

| Recording Time (seconds) | Geo-electrical Potential Changes recorded (mV) | | |
|---|---|---|---|
| | Station A | Station B | Station C |
| 0 | 35 | 25 | 65 |
| 1 | 50 | 15 | 45 |
| 2 | 10 | 35 | 75 |
| 3 | 60 | 25 | 45 |
| 4 | 25 | 55 | 95 |
| 5 | 10 | 30 | 35 |
| 6 | 105 | 85 | 120 |
| 7 | 11 | 35 | 55 |
| 8 | 60 | 75 | 130 |
| 9 | 135 | 105 | 155 |
| 10 | 60 | 75 | 45 |
| 11 | 250 | 35 | 85 |
| 12 | 85 | 85 | 175 |
| 13 | 148 | 140 | 65 |
| 14 | 100 | 75 | 195 |
| 15 | 135 | 355 | 55 |
| 16 | 105 | 150 | 220 |
| 17 | 120 | 45 | 55 |
| 18 | 85 | 145 | 405 |
| 19 | 100 | 55 | 175 |
| 20 | 75 | 30 | 55 |
| 21 | 85 | 75 | 155 |
| 22 | 55 | 25 | 55 |
| 23 | 55 | 55 | 130 |
| 24 | 55 | 35 | 40 |
| 25 | 45 | 45 | 105 |
| 26 | 35 | 65 | 25 |
| 27 | 45 | 55 | 65 |
| 28 | 25 | 35 | 15 |
| 29 | 20 | 50 | 35 |
| 30 | 15 | 25 | 10 |

## REFERENCES

1. Adetoyinbo, A.A., Popoola, O.I., Hammed, O.S., and Adeniran, A.A. 2008. "Fabrication of a Portable ULF Signal Receiver for Monitoring Electromagnetic Earthquake Precursors". *Online Journal of Earth Sciences*. 2(4): 113-117.

2. AL-saigh, N.H., Mohammed, Z.S., and Dahham, M.S. 1994. "Detection of Water Leakage from Dams by Self-Potential Method". *Eng. Geol.* 37: 115-121.

3. Atkinson, B.K. 1982. "Sub-critical Crack Propagation in Rocks: Theory, Experimental Results and Applications". *J. Struct. Geol.* 4: 41 – 56.

4. Atkinson, B.K. 1984. "Subcritical Crack Growth in Geological Materials". *J. Geophys. Res.* 89 (B6): 4077– 4114.

5. Atkinson, B.K. and Meredith, P.G. 1987. "The Theory of Subcritical Crack Growth with Application to Minerals and Rocks". In: *Fracture Mechanics of Rock*. 111 – 166. Atkinson, B. (ed). Academic Press: London, UK.

6. Ayling, M.R., Meredith, P.G., and Murrell, S.A.F. 1995. "Microcracking During Triaxial Deformation of Porous Rocks Monitored by Changes in Rock Physical Properties, I. Elastic Wave Propagation Measurements on Dry Rocks". In: C.J. Spiers and T. Takeshita (eds). *Influence of Fluids on*

*Deformation Processes in Rocks. Tectonophys.* 245,195- 211.

7. Batzle, M.L., Simmons, G., and Siegfried, R.W. 1980. "Microcrack Closure in Rocks under Stress: Direct Observation". *J. Geophys. Res.* 85 (B12): 7072-7090.

8. Bernabé, Y. and Bruderer, C. 1998. "Effect of the Variance of Pore Size Distribution on the Transport Properties of Heterogeneous Networks". *J. Geophys. Res.* 103 (B1): 513-525.

9. Berryman, J.G. 1992a. "Exact Effective Stress Rules in Rock Mechanics". *Phys. Rev. A.* 46(6): 3307-3311.

10. Berryman, G. 1992b. "Effective Stress for Transport Properties of Inhomogeneous Porous Rock." *J. Geophys. Res.* 97:17409-17424.

11. Boore, D.M. and J. Boatwright. 1984. "Average Body-Wave Radiation Coefficients". *Bull. Seismol. Soc. Am.*, 74 (5): 1,754-1,782.

12. Brown, S.R. and Scholz, C.H. 1985a. "Broad Bandwidth Study of the Topography of Natural Rock Surfaces". *J. Geophys. Res.* 90: 12,575 – 12,582.

13. Brown, S.R. and Scholz, C.H. 1986. "Closure of Rock Joints". *J. Geophys. Res.* 91: 4939 – 4948.

14. Brune, J.N. 1970. "Tectonic Stress and the Spectra of Seismic Shear Waves from Earthquakes". *J. Geophys. Res.*, 75(4):997-5,009.

15. Byerlee, J. 1993. "Model for Episodic Flow of High Pressure Water in Fault Zones before Earthquakes". *Geology* 21: 303 – 306

16. Corwin, R.F. and Morrison, H.F. 1977. "Self-Potential Variations Preceding Earthquakes in Central California". *Geophys. Res. Letts.* 4(4): 171-174

17. David, C. 1993. "Geometry of Flow Paths for Fluid Transport in Rocks". *J. Geophys. Res.* 98, B7, 12,267-12,278.

18. Derr, J.S. 1973. "Earthquake Lights: A review of Observations and Present Theories". *Bull. Seismol. Soc. Am.* 63: 2177 - 2187

19. Dunn, D.E., Lafountain, L.J., and Jackson, R.E. 1973. "Porosity Dependence and Mechanism of Brittle Fracture in Sandstones". *J. Geophys. Res.* 78(14):2403 - 2417

20. Enescu, B. and K. Ito. 2001. "Some Premonitory Phenomena of the 1995 Hyogo-Ken Nanbu (Kobe) Earthquake: Seismicity, B-Value and Fractal Dimension". *Tectonophysics*, 338 (3-4): 297-314.

21. Enescu, B. and K. Ito. 2002. "Spatial Analysis of the Frequency-Magnitude Distribution and Decay Rate of the 2000 Western Tottori Earthquake". *Earth Planets Space.* 54(8): 847-860.

22. Fajklewicz, Z. and K. Jakiel. 1989. "Induced Gravity Anomalies and Seismic Energy as a Basis for Prediction of Mining Tremors". *PAGEOPH.* 129 (3/4): 536-552.

23. Fenoglio, M.A., Johnston, M.J.S., and Byerlee, J.D. 1995. "Magnetic and Electric Fields Associated with Changes in High Pore Pressure in Fault Zones: Application to the Loma Prieta ULF Emissions". *J. Geophys. Res.* 100 (B7): 12,951-12,958

24. Freiman, S.W. 1984. "Effects of Chemical Environments on Slow Crack Growth in Glasses and Ceramics". *J. Geophys. Res.* 89 (B6): 4072 – 407.

25. Glover, P.W.J., Matsuki, K., Hikima, R., and Hayashi, K. 1998. "Synthetic Rough Fractures in Rocks". *J. Geophys. Res.* 103 (B5): 9609 – 9620.

26. Haartsen, M.W., Dong, W., and Toksöz, M.N. 1998. "Dynamic Streaming Currents from Seismic Point Sources in Homogeneous Poroelastic Media. *Geophys. J. Int.* 132: 256- 274.

27. Holub, K. 1996. "Space-Time Variations of the Frequency-Energy Relation for Mining Induced Seismicity in the Ostrava-Karvina Mining District". *PAGEOPH.* 146: 265-280.

28. Huang, Q., A.O. Oncel, and G.A. Sobolev. 2002. "Precursory Seismicity Changes Associated with the Mw=7.4 1999 August 17 Izmit (Turkey) Earthquake". *Geophys. J. Int.*, 151: 235-242.

29. Hubbert, M.K. and Rubey, W.W. 1959. "Role of Fluid Pressure in Mechanics of Overthrust Faulting. I. Mechanics of Fluid Filled Porous Solids and its Application to Overthrust Faulting". *Bull. Geol. Soc. Am.* 70:115 – 166.

30. Jaeger, J.C. and Cook, N.G.W. 1979. *Fundamentals of Rock Mechanics (3rd edition).* Chapman and Hall: London, UK. 593.

31. Kanamori, H. 1981. "The Nature of Seismic Patterns before large Earthquakes". In: *Earthquake Prediction: An International Review.* Simpson, D.W. and Richards, P.G.(eds.). Maurice Ewing Series. Vol.4, AGU: Washington D.C., pp. 1-19.

32. Katz, A.J. and Thompson, A.H. 1985. "Fractal Sandstone Pores: Implication for Conductivity and Pore Formation". *Phys. Rev. Lett.* 54:1325 – 1328.

33. Katz, A.J. and Trugman, S.A. 1988. "Residual Water Saturation, Electrical Conductivity and Rough Rock/Pore Interfaces". *J. Colloid Int. Sci.* 123: 8-13.

34. Keaney, G.M. 1998. "Evolution of Permeability in Low Porosity Rocks Under Simulated Crustal Stress Conditions". Ph.D. Thesis, University of London.

35. Kligfield, R., Hunziker, J., Dallmeyer, R.D., and Schamel, S. 1986. *Jour. Struct. Geol.* 8: 781-798.

36. Melnikov, N.N., A.A. Kozyrev, and V.I. Panin. 1996. "Induced Seismicity in Large Scale Mining in the Kola Peninsula and Monitoring to Reveal Informative Precursors. *PAGEOPH.* 147 (2): 263-276.

37. Mendecki, A.J., G. van Aswegen, J.N.R. Brown, and P. Hewlett. 1990. *The Welcom Seismological Network, Proc. 2nd International Symposium on Rockburst and Seismicity in Mines*: Minneapolis, MN. 367-377.

38. Mendecki, A.J., A. van Z. Brink, R.W.E. Green, P. Mountfort, A. Dzhafarov, J. Niewiadomski, A. Kijko, M. Sciocatti, S. Radu, G. van Aswegen, P. Hewlett, E. de Kock, and T. Stankiewicz. 1996. "Seismology for Rockbursts Prevention, Control, and Prediction". SIMRAC report. ISS International Limited. 309.

39. Meredith, P.G., Main, I., and Jones, C.J. 1990. "Temporal Variations in Seismicity During Quasi-Static and Dynamic Rock Failure". *Tectonophys.* 175: 249 – 268.

40. Monterroso, D. 2003. "Statistical Seismology Studies in Central America: B-Value, Seismic Hazard and Seismic Quiescence". *Compr. Summaries Uppsala Diss. Fac. Sci. Technol.* 897: 27 Acta Univ. Upsaliensis: Uppsala, Sweden.

41. Nuannin, P., O. Kulhánek, and L. Persson. 2005. "Spatial and Temporal B-Value Anomalies Preceding the Devastating off coast of NW Sumatra Earthquake of December 26, 2004". *Geophys. Res. Lett.* 32: L11307, doi:10.1029/2005GL0 22679.

42. Nur, A. and Byerlee, J.D. 1971. "An Exact Effective Stress Law for Elastic Deformation of Rock with Fluids". *J. Geophys. Res.* 76: 6414 – 6419.

43. Ranalli, G. 1995, \Rheology of the Earth. Chapman and Hall: London, UK. 413.

44. Ruffet, C., Darot, M. and Gueguen, Y. 1995. "Surface Conductivity in Rocks: A Review". *Surv. Geophys.* 16: 83 – 105.

45. Sibson, R.H. 1980. "Power Dissipation and Stress Levels on Faults in the Upper Crust. *J. Geophy. Res.* 85: 6239 – 6247.

46. Scheidegger, A.E. 1974. *The Physics of Flow Through Porous Media*. Univ. of Toronto Press: Toronto, Ont., Canada. 353.

47. Scholz, C.H. 1996. *The Mechanics of Earthquakes and Faulting*. Cambridge University Press: London, UK. 439.

48. Schorlemmer, D., G. Neri, S. Wiemer, and A. Mostaccio. 2003. "Stability and Significance Tests for B-Values Anomalies: Example from the Tyrrhenian Sea". *Geophys Res. Lett.* 30 (16): 1835, doi10.1029 /2003GL017335.

49. Schorlemmer, D., S. Wiemer, and M. Wyss. 2004. "Earthquake Statistics at Parkfield I: Stationarity of B-Values". *J. of Geophys. Res.* 109, B12307, doi10.1029 /2004- JB003234.

50. Trimmer, D., Bonner, B., Heard, H. C. and Duba, A. 1980. "Effect of Pressure and Stress on Water Transport in Intact and Fractured Gabbro and Granite". *J. Geophys. Res.* 85 (B12), 7059 – 7071.

51. Tsang, Y.W. and Witherspoon, P.A. 1981. "Hydromechanical Behaviour of a Deformable Rock Fracture Subject to Normal Sress". *J. Geophys. Res.* 86: 9287 – 9298.

52. Walsh, J.B. and Brace, W.F. 1984. "The Effect of Pressure on Porosity and the Transport Properties of Rock". *J. Geophys. Res.* 89: 9425 – 9431.

53. Warwick, J.W., Stoker, C., and Meyer, T.R. 1982. "Radio Emission Associated with Rock Fracture: Possible Application to the great Chilean Earthquake of May 22, 1960". *J. Geophys. Res.* 87: 2851 – 2859.

54. Wyss, M. and A.H. Martirosyan. 1998. Seismic Quiescence Before the M 7, 1988, Spitak Earthquake, Armenia". *Geophys. J. Int.*, 134(2), 329-340.

55. Yoshida, S., Manjgaladze, P., Zilpimiani, D., Ohnaka, M., and Nakatani, M. 1994. "Electromagnetic Emissions Associated with Frictional Sliding of Rock". In: *Electromagnetic Phenomena Related to Earthquake Prediction*. Hayakawa, M. and Fujinawa, Y. (eds.). Terrapub, Tokyo, Japan. 307 – 322.

56. Yoshida, S., Uyeshima, M., and Nakatani, M. 1997. "Electric Potential Changes Associated with

Slip Failure of Granite: Preseismic and Coseismic Signals". *J. Geophys. Res.* 102 (B7), 14883 – 14897.

57. Zhu, W. and Wong, T.F. 1996. "Permeability Reduction in a Dilating Rock: Network Modelling of Damage and Tortuosity". *Geophys. Res. Lett.* 23(22): 3099 – 3102

58. Zoback, M.D. and Byerlee, J.D. 1975. "The Effect of Microcrack Dilatancy on the Permeability of Westerly Granite". *J. Geophys. Res.* 80(5): 752 – 755.

## SUGGESTED CITATION

Adetoyinbo, A.A., O.I. Popoola, O.S. Hammed, and L.A. Sumonu. 2009. "Detection of Seismic ULF Geo-Electrical Potential Variations as a Tremor Precursor". *Pacific Journal of Science and Technology*. 10(1):540-555.

Pacific Journal of Science and Technology